Regioselective Double Cycloplatination of 9,10-Bis(diphenylphosphino)anthracene

Jian Hu and John H. K. Yip*

Department of Chemistry, National University of Singapore, 3 Science Drive 3, Singapore, 117543

Received April 21, 2008

Double cyclometalation of 9,10-bis(diphenylphosphino)anthracene (PAnP) by $Pt(L)(OTf)_2$ (L = diphosphines, OTf = CF_3SO_3) gives rise to the geometrical isomers *syn*- and *anti*-$[Pt_2(L)_2(PAnP\text{-}H_2)](OTf)_2$ (**Pt_2**). The reaction is regioselective, with the *syn*-isomer being the kinetic product. The cyclomelation is reversible, and thermodynamic product distribution is obtained after prolonged standing. The ratio of the isomers is subject to the influence of solvents and ancillary diphosphines. Protonolysis of the Pt−C leads to a monocyclometalated intermediate. A mechanistic postulate that invokes a preferential *electrophilic* attack of the Pt ions at the C−H bonds of the anthracenyl ring is proposed to explain the regioselectivity.

Introduction

Cyclometalation is a facile and common way to convert a C−H bond to a metal−carbon bond.[1] The reaction begins with coordination of a metal atom to a ligand (i.e., phosphines and amines) that has pendent alkyl or aryl groups, followed by cleavage of a C−H bond in a pendent aryl or alkyl group, and finally formation of metal−carbon bond and metallacycle. The mechanisms proposed for the C−H bond activation are electrophilic attack, nucleophilic addition, and σ-bond metathesis.[1c]

Regioselective cyclometalation could happen to ligands that have more than one C−H bond that is reactive toward the incoming metal atom.[2] Ryabov[1c] classified regioselective cyclometalation into enforced regioselectivity, which is dictated by electronic or steric factors, and regulated regioselectivity, which can be altered by changing reaction conditions. Understanding the origin of regioselectivity not only is an important step toward synthetic application[3] of the reaction but also provides insights into important problems such as C−H bond and metal−ligand activations.

Double cyclometalation is possible for ligands that have two donor groups and more than one activated C−H bond.[1c,2a−q] The reaction can produce geometrical isomers, and their yields could be different if the attack of the second metal atom is regioselective. The origin of regioselectivity in double cyclometalation is an intriguing problem. The first question is whether the first metal atom directs and activates/deactivates the second attack. It is related to the mechanism of the C−H bond cleavage and metal−ligand interactions. Another question concerns electronic, steric, and solvent effects on the regioselectivity, which is related to the question of whether the reaction is kinetically or thermodynamically controlled. So far our understanding of regioselectivity of double cyclometalation is rather limited, despite the fact that it was first observed by Trofimenko more than 30 years ago.[2a] Subsequent studies on double cyclometalation of 1,4-disubstituted benzenes showed that the *para*-dimetalation is favored over *ortho*-dimetalation mainly due to steric factors.[2a−q] Notably, Steel reported a systematic investigation of double cyclopalladation of a series of bis(2-pyridyloxy)-napthalenes,[2c,g] showing that the reaction is kinetically controlled, but thermodynamic products could be obtained at high temperature.

Recently we reported the syntheses and electronic spectroscopy of the doubly cycloplatinated complexes $[Pt_2(L)_2(PAnP\text{-}H_2)](OTf)_2$ (**Pt_2**) (L = bis(diphenylphosphino)methane (dppm), 1,2-bis(diphenylphosphino)ethane (dppe), 1,3-bis(diphenylphosphino)propane (dppp), PAnP = 9,10-bis(diphenylphosphino)anthracene) (Scheme 1).[4] Our further study showed that the double cyclometalation of PAnP by $Pt^{II}(L)(OTf)_2$ is very fast, producing two geometrical isomers, *syn*- and *anti*-**Pt_2**. The second cycloplatination is found to be regioselective, and the selectivity depends on solvent and L. Reported in this paper is our effort

* Correspondence author. E-mail: chmyiphk@nus.edu.sg. Fax: 65-67791691.

(1) (a) Kleiman, J. P.; Dubeck, M. *J. Am. Chem. Soc.* **1963**, *85*, 1544. (b) Chatt, J.; Davidson, J. M. *J. Chem. Soc.* **1965**, 843. (c) Ryabov, A. D. *Chem. Rev.* **1990**, *90*, 403. (d) Canty, A. J.; van Koten, G. *Acc. Chem. Res.* **1995**, *28*, 406. (e) Newkome, G. R.; Puckett, W. E.; Gupta, V. K.; Kiefer, G. E. *Chem. Rev.* **1986**, *86*, 451. (f) Dehand, J.; Pfeffer, M. *Coord. Chem. Rev.* **1976**, *18*, 327. (g) Newkome, G. R.; Puckett, W. E.; Gupta, V. K.; Kiefer, G. E. *Chem. Rev.* **1986**, *86*, 451. (h) Omae, I. *Organometallic Intramolecular-Coordination Compounds*; Elsevier: Amsterdam, 1986. (i) Bruce, M. I. *Angew. Chem., Int. Ed. Engl.* **1977**, *16*, 73.

(2) (a) Trofimenko, S. *J. Am. Chem. Soc.* **1971**, *93*, 1808. (b) Trofimenko, S. *Inorg. Chem.* **1973**, *12*, 1215. (c) Hartshorn, C. M.; Steel, P. J. *Organometallics* **1998**, *17*, 3487. (d) Steenwinkel, P.; James, S. L.; Grove, D. M.; Kooijman, H.; Spek, A. L.; van Koten, G. *Organometallics* **1997**, *16*, 513. (e) van der Boom, M. E.; Liou, S.-Y.; Shimon, L. J. W.; Ben-David, Y.; Milstein, D. *Organometallics* **1996**, *15*, 2562. (f) Slater, J. W.; Lydon, D. P.; Alcock, N. W.; Rourke, J. P. *Organometallics* **2001**, *20*, 4418. (g) O'Keefe, B. J.; Steel, P. J. *Organometallics* **2003**, *22*, 1281. (h) Sumby, C. J.; Steel, P. J. *Organometallics* **2003**, *22*, 2358. (i) Philips, I. G.; Steel, P. G. *J. Organomet. Chem.* **1991**, *410*, 247. (j) Frenández, A.; Frenández, J. J.; López-Torres, M.; Suárez, A.; Ortigueira, J. M.; Vila, J. M.; Adams, H. *J. Organomet. Chem.* **2000**, *612*, 85. (k) Crespo, M.; Grande, C.; Klein, A. *J. Chem. Soc., Dalton Trans.* **1999**, 1629. (l) Zucca, A.; Doppiu, A.; Cinellu, M. A.; Stoccoro, S.; Minghetti, G.; Manassero, M. *Organometallics* **2002**, *21*, 783. (m) Vicente, J.; Abad, J. A.; Rink, B.; Hernandez, F. S.; Arellano, M. C. *Organometallics* **1997**, *16*, 5269. (n) Cardenas, D. J.; Echavarren, A. M.; Ramirez de Arellano, M. C. *Organometallics* **1999**, *18*, 3337. (o) Vicente, J.; Saura-Llamas, I.; Cuadrado, J.; Ramirez de Arellano, M. C. *Organometallics* **2003**, *22*, 5513. (p) Chakladar, S.; Paul, P.; Mukherjee, A. K.; Dutta, S. K.; Nanda, K. K.; Podder, D.; Nag, K. *J. Chem. Soc., Dalton Trans.* **1992**, 3119. (q) Chakladar, S.; Paul, P.; Venkatsubramanian, K.; Nag, K. *J. Chem. Soc., Dalton Trans.* **1991**, 2669. (r) Holland, A. W.; Bergman, R. G. *Organometallics* **2002**, *21*, 2149.

(3) (a) Ritleng, V.; Sirlin, C.; Pfeffer, M. *Chem. Rev.* **2002**, *102*, 1731. (b) Moritani, I.; Fujiwara, Y. *Tetrahedron Lett.* **1967**, 1119. (c) Murai, S.; Kakiuchi, F.; Sekine, S.; Tanaka, Y.; Kamatani, A.; Sonoda, M.; Chatani, N. *Nature* **1993**, *366*, 529. (d) Hull, K. L.; Sanford, M. S. *J. Am. Chem. Soc.* **2007**, *129*, 11904.

(4) Hu, J.; Lin, R.; Yip, J. H. K.; Wong, K.-Y.; Ma, D.-L.; Vittal, J. J. *Organometallics* **2007**, *26*, 6533.

10.1021/om800356k CCC: $40.75
Publication on Web 01/27/2009

Scheme 1

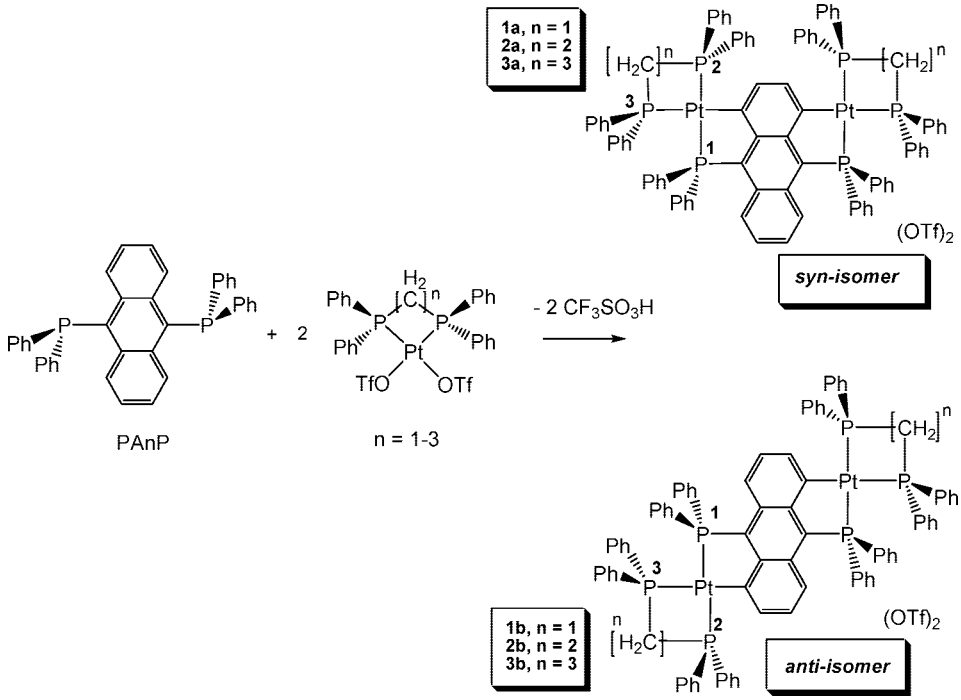

Scheme 2

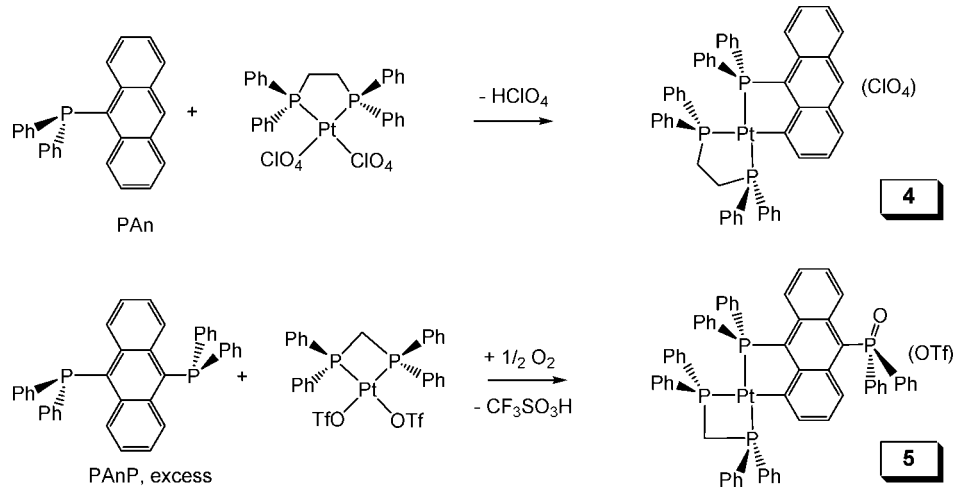

to understand the regioselectivity of the double cyclometalation. Two singly metalated complexes, [Pt(dppe)(PAn-H)]ClO_4 (**4**) (PAn = 9-(diphenylphosphino)anthracene) and [Pt(dppm)(PAnPO-H)]OTf (**5**) (PAnPO is singly oxidized PAnP) (Scheme 2), serve as models for the singly cyclometalated intermediate that precedes the second metalation.

Experimental Section

General Methods. All syntheses were carried out in a N_2 atmosphere unless stated otherwise. All the solvents used for synthesis were purified according to the literature procedures. Triflic acid was purchased from Sigma-Aldrich. **1a**, **1b**, **2a**, **2b**, **3a**, **3b**, **4**,[4] 9,10-bis(diphenylphosphino)anthracene (PAnP),[5] and 9-(diphenylphosphino)anthracene (PAn)[6] were prepared according to the reported methods. Pt(L)$(OTf)_2$[7] were prepared in situ by reacting Pt(L)Cl_2 with 2 molar equiv of AgOTf in CH_3CN/CH_2Cl_2 based on modified literature methods.

Physical Measurements. NMR experiments were performed on a Bruker ACF 300, AMX500, or DRX500 spectrometer. All chemical shifts (δ) are reported in ppm and coupling constants (J) in Hz. ^{1}H NMR chemical shifts are relative to TMS; the resonance of residual protons of solvents was used as an internal standard. $^{31}P\{^1H\}$ NMR chemical shifts were relative to 85% H_3PO_4 in D_2O. Electrospray ionization mass spectra (ESI-MS) were measured on a Finnigan MAT 731 LCQ spectrometer. Elemental analyses of the complexes were carried out at the Elemental Analysis Laboratory at the National University of Singapore.

Synthesis of [Pt(dppm)(PAnPO-H)](OTf) (5). A CH_2Cl_2 solution (70 mL) of Pt(dppm)$(OTf)_2$ (568 mg, 0.647 mmol) was added slowly into a CH_2Cl_2 solution (100 mL) of excess PAnP (1.42 g,

(5) Yip, J. H. K.; Prabhavathy, J. *Angew. Chem., Int. Ed.* **2001**, *40*, 2159.
(6) Wesemann, J.; Jones, P. G.; Schomburg, D.; Heuer, L.; Schmutzler, R. *Chem. Ber.* **1992**, *125*, 2187.
(7) (a) Anderson, G. K.; Davies, J. A.; Schoeck, D. J. *Inorg. Chim. Acta* **1983**, *76*, L251. (b) Fallis, S.; Anderson, G. K.; Rath, N. P. *Organometallics* **1991**, *10*, 3180. (c) Stang, P. J.; Cao, D. H.; Saito, S.; Arif, A. M. *J. Am. Chem. Soc.* **1995**, *117*, 6273.

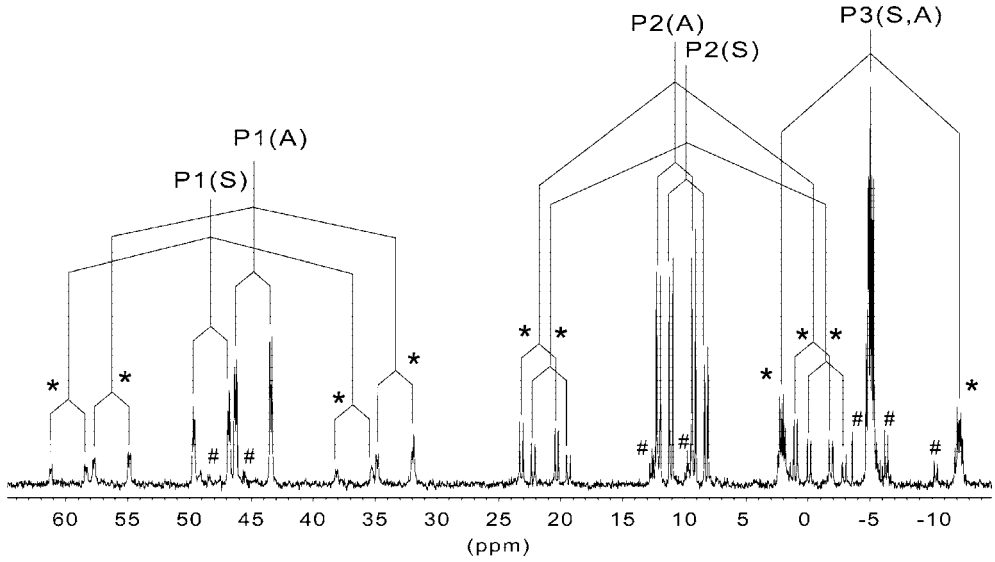

Figure 1. $^{31}P\{^1H\}$ NMR (121.5 M, CD_3CN) spectrum of the crude product of reaction 3 in CH_2Cl_2 (S: *syn*-isomer; A: *anti*-isomer). * ^{195}Pt satellites, # minor unknown.

2.60 mmol). After stirring for 2 h, all solvent was removed by rotoevaporation to give a yellow solid. (The following purifying process was carried out in air.) The solid was extracted with CH_3CN to remove the unreacted PAnP, which was not soluble in CH_3CN. Removal of CH_3CN by rotoevaporation gave a yellow solid. Slow diffusion of Et_2O into a CH_2Cl_2 solution of the solid gave a mixture of needle- and block-shaped yellow crystals. The needle-shaped crystals were carefully removed and discarded, and the remaining block crystals were regrown. This process was repeated several times to obtain pure compound **5**. Single crystals suitable for X-ray diffraction were grown by slow diffusion of Et_2O into a CH_3CN solution of the purified complex. Anal. Calcd (%) for **5**·$2H_2O$, $C_{64}H_{53}F_3O_6P_4PtS$: C, 57.97; H, 4.03. Found (%): C, 57.85; H, 4.05. ^1H NMR (500 MHz, CD_3CN, δ/ppm): 8.78−8.77 (m, 1H, H_5, An), 8.34−8.33 (m, 1H, H_4, An), 7.86−7.85 (m, 1H, H_8, An), 7.80−7.76 (m, 4H, Ph), 7.69−7.68 (m, 1H, H_2, An), 7.67−7.63 (m, 4H, Ph), 7.56−7.54 (m, 8H, Ph), 7.46−7.45 (m, 10H, Ph), 7.36−7.29 (m, 6H, Ph), 7.19−7.17 (m, 2H, $H_{6,7}$, An), 7.14−7.12 (m, 8H, Ph), 6.81−6.78 (m, 1H, H_3, An), 4.85−4.81 (m, 2H, CH_2). $^{31}P\{^1H\}$ NMR (121.5 MHz, CD_3CN, δ/ppm): 44.71 (ddd, P_1), 31.23 (d, P_4), −21.99 (dd, P_2), −29.81 (dd, P_3); $^1J(P_1-Pt) = 2807$ Hz, $^1J(P_2-Pt) = 2418$ Hz, $^1J(P_3-Pt) = 1424$ Hz; $^2J(P_1-P_2) = 361$ Hz, $^2J(P_1-P_3) = 12$ Hz, $J(P_2-P_3) = 39$ Hz, $J(P_1-P_4) = 4$ Hz. ESI-MS(*m*/*z*): 1140.4 $[M - OTf]^+$.

Protonolysis of Pt_2. In a typical reaction, about 25 mg of the **Pt_2** complexes was dissolved in ∼0.5 mL of CD_2Cl_2 in a NMR tube to give a yellow solution. A slight excess of HOTf was then added dropwise until a dark red mixture was obtained, and ^1H and $^{31}P\{^1H\}$ NMR spectra of the mixture were recorded.

X-ray Crystallography. The diffraction experiments were carried out on a Bruker AXS SMART CCD 3-circle diffractometer with a sealed tube at 23 °C using graphite-monochromated Mo Kα radiation ($\lambda = 0.71073$ Å). The software used were SMART[8a] for collecting frames of data, indexing reflections, and determination of lattice parameters; SAINT[8a] for integration of intensity of reflections and scaling; SADABS[8b] for empirical absorption correction; and SHELXTL[8c] for space group determination, structure solution, and least-squares refinements on F^2. The crystals were mounted at the end of glass fibers and used for the diffraction experiments. Anisotropic thermal parameters were refined for rest of the non-hydrogen atoms. The H atoms were placed in their ideal positions. A brief summary of crystal data and experimental details are given in the Supporting Information.

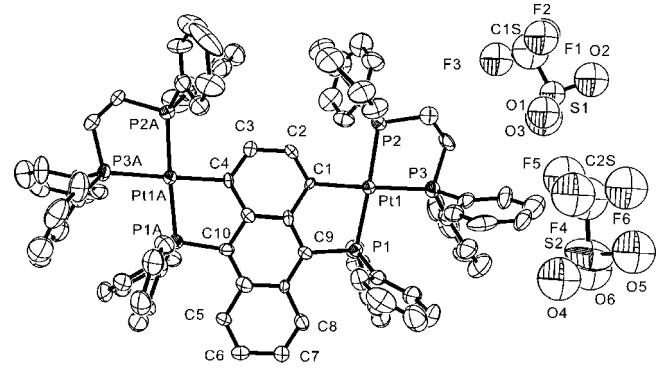

Figure 2. ORTEP diagram of **2a** (50% thermal ellipsoids). H atoms and solvent molecules are omitted for clarity.

Results and Discussion

Reactions and Characterizations of Products. In the following discussion, the cyclometalation reactions of PAnP and $Pt(dppm)(OTf)_2$, $Pt(dppe)(OTf)_2$, and $Pt(dppp)(OTf)_2$ are referred to as reactions 1, 2, and 3, respectively. The structures of **1a**, **1b**, **3a**, **3b**, and **4** were reported in our previous paper.[4] The $^{31}P\{^1H\}$ NMR spectra of the products isolated from the three reactions show two sets of first-order signals with some of the peaks partly overlapped. A typical spectrum is shown in Figure 1, which shows $^{31}P\{^1H\}$ NMR signals of the crude product of the reaction 3.

The spectrum is dominated by two sets of intense signals and small peaks of some minor unknown compounds. The chemical shifts, J_{P-P} and $^1J_{Pt-P}$, are listed in Table ST1. Of the two sets of intense signals, each of them comprises three mutually coupled double doublets with an intensity ratio of 1:1:1. That all the P atoms coordinate to Pt atoms is evident from the $^1J_{Pt-P}$ satellites of the signals. On the other hand, the two sets of signals do not couple with each other. This indicates that the reactions produce two Pt complexes in which the metal centers are coordinated to three different P atoms. The assignments of the signals have been reported.[5] In summary, the signals that show large $^2J_{P-P}$ coupling constants (343−361 Hz) are assigned to P1 and P2, while the ones with small $^2J_{P-P}$ (4−39 Hz) are attributed to P3 (see Scheme 1 for the labels of the P

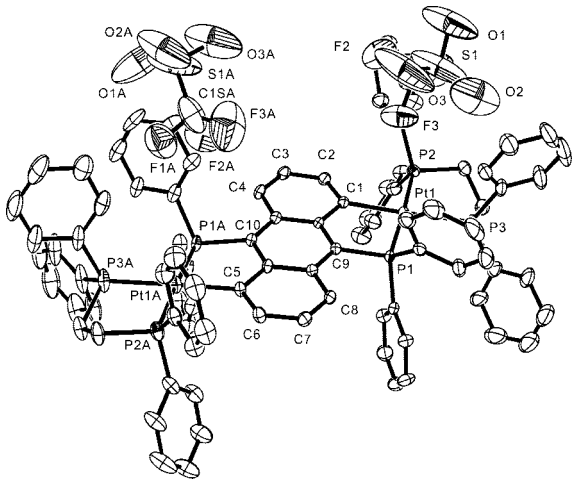

Figure 3. ORTEP diagram of **2b** (50% thermal ellipsoids). H atoms and solvent molecules are omitted for clarity.

Table 1. Selected Bond Lengths (Å) and Angles (deg) for $2a \cdot 1.25(CH_2Cl_2)0.5(Et_2O)$

Pt(1)−P(1) 2.281(3)	P(1)−Pt(1)−P(2) 176.19(11)
Pt(1)−P(2) 2.328(4)	P(1)−Pt(1)−P(3) 99.47(12)
Pt(1)−P(3) 2.313(4)	P(2)−Pt(1)−P(3) 83.83(13)
Pt(1)−C(1) 2.106(1)	P(1)−Pt(1)−C(1) 82.4(3)
	P(2)−Pt(1)−C(1) 94.4(3)

Table 2. Selected Bond Lengths (Å) and Angles (deg) for $2b \cdot 2CH_2Cl_2$

Pt(1)−P(1) 2.2816(15)	P(1)−Pt(1)−P(2) 176.90(5)
Pt(1)−P(2) 2.3175(16)	P(1)−Pt(1)−P(3) 99.67(6)
Pt(1)−P(3) 2.3234(16)	P(2)−Pt(1)−P(3) 82.99(6)
Pt(1)−C(1) 2.073(5)	P(1)−Pt(1)−C(1) 82.54(15)
	P(2)−Pt(1)−C(1) 94.82(15)
	P(3)−Pt(1)−C(1) 177.76(15)

atoms).[9] The two sets of signals are attributed to the geometrical isomers *syn*- and *anti*-$[Pt_2(L)_2(PAnP\text{-}H_2)](OTf)_2$. The assignment is confirmed by the spectra of pure samples of the complexes. The most important message obtained from the spectra is that two geometrical isomers are produced in the reactions and the double cyclometalation is clearly regioselective, as the yields of the isomers are different in all three reactions.

Reacting $Pt(dppe)(ClO_4)_2$ with 1 molar equiv of 9-(diphenylphosphino)anthracene (PAn) gives the mononuclear cyclometalated complex $[Pt(dppe)(PAn\text{-}H)](ClO_4)$ (**4**), which has been fully characterized. The reaction of $Pt(dppm)(OTf)_2$ and excess PAnP gives the singly cyclometalated [Pt(dppm)(PAnP-H)](OTf) together with the doubly cyclometalated complexes (**1a** and **1b**). When exposed to air, the uncoordinated P atom in [Pt(dppm)(PAnP-H)](OTf) is oxidized and the complex Pt(dppm)(PAnPO-H)](OTf) (**5**) is formed. The $^{31}P\{^1H\}$ NMR spectrum of **5** consists of four sets of signals (P1−P4) of equal intensity. The chemical shifts and signal patterns of the three P atoms (P1, P2, and P3) coordinating to the Pt ion are similar to those of **1a**, except that P1 is further coupled to the oxidized P4 with a very small coupling constant of ∼4 Hz. Because of its long-range coupling to P1, P4 appears as a doublet at δ 31.

(8) (a) *SMART & SAINT Software Reference Manuals*, version 4.0; Siemens Energy & Automation, Inc., Analytical Instrumentation: Madison, WI, 1996. (b) Sheldrick, G. M. *SADABS: A Software for Empirical Absorption Correction*; University of Gottingen: Gottingen, Germany, 1996. (c) *SHELXTL Reference Manual*, version 5.03; Siemens Energy & Automation, Inc., Analytical Instrumentation: Madison, WI, 1996.

(9) (a) Allen, F. H.; Pidcock, A. *J. Chem. Soc. A* **1968**, 2700. (b) Appleton, T. G.; Clark, H. C.; Manzer, L. E. *Coord. Chem. Rev.* **1973**, *10*, 335.

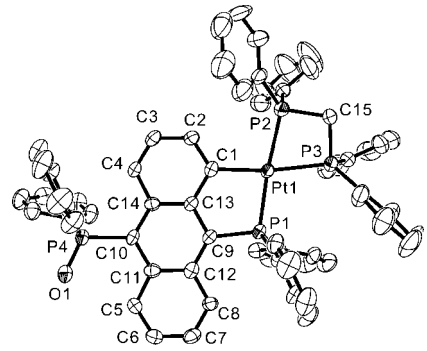

Figure 4. ORTEP diagrams of the cation of **5** (50% thermal ellipsoids). H atoms, solvent, and the anion are omitted for clarity.

Table 3. Selected Bond Lengths (Å) and Angles (deg) for $5 \cdot 0.5H_2O$

Pt(1)−P(1) 2.255(18)	P(1)−Pt(1)−P(2) 174.68(6)
Pt(1)−P(2) 2.316(2)	P(1)−Pt(1)−P(3) 103.82(7)
Pt(1)−P(3) 2.330(2)	P(2)−Pt(1)−P(3) 71.00(7)
Pt(1)−C(1) 2.052(7)	P(1)−Pt(1)−C(1) 83.9(2)
P(2)−O(1) 1.473(6)	P(2)−Pt(1)−C(1) 101.3(2)
	P(3)−Pt(1)−C(1) 172.2(2)

Structures. The geometrical isomers can be separated by fractional crystallization. The X-ray crystal structures of **1a**, **3a**, and **3b** have been previously reported by us. Figures 2 and 3 show the structures of *syn*-$[Pt_2(dppe)_2(PAnP\text{-}H_2)](OTf)_2 \cdot 1.25CH_2Cl_2 \cdot 0.5Et_2O$ (**2a** $\cdot 1.25CH_2Cl_2 \cdot 0.5Et_2O$) and *anti*-$[Pt_2(dppe)_2(PAnP\text{-}H_2)](OTf)_2 \cdot 2CH_2Cl_2$ (**2b** $\cdot 2CH_2Cl_2$), which are representatives for the *syn*- and *anti*-isomers. Selected bond distances and angles are listed in Tables 1 and 2. The structure of **2a** shows two *syn*-oriented Pt centers attached to the C1 and C4 positions of the anthracenyl ring, while the C1 and the C5 positions are metalated in the *syn*-isomers **2b**. The *syn*- and *anti*-isomers display approximate C_{2v} and C_{2h} symmetry, respectively. The Pt−P and Pt−C bond lengths are typical for cyclometalated Pt-phosphine complexes.[4] The anthracenyl rings of the complexes are nearly planar. The metal center is the center of two five-membered chelated rings that comprise the P atoms of dppe and PAnP, as well as the substituted C atom. The bite angles P2−Pt1−P3 for the complexes (**2a** 83.83(13)°, **2b** 82.99(6)°) are significantly smaller than that of **3a** (87.49(5)°) and **3b** (86.88(5)°) but larger than that of **1a** (70.74(6)°).

Complex **4** is a mononuclear analogue of **2a** and **2b**. It consists of a Pt ion attached to the anthracenyl ring at the C1 position.[4] The coordination geometry and Pt−C and Pt−P bond lengths are similar to those of **2a** and **2b**.

The structure of **5** is shown in Figure 4 (Table 3 for selected bond distances and angles). One of two P atoms (P1) on PAnP is coordinated to a Pt ion, which is attached to the C1 position of anthracene. The coordination geometry of the Pt center and the Pt−C and Pt−P bond lengths are similar to those of **1a**. The other P atom on PAnP is oxidized to phosphine oxide. The P═O bond distance (1.473(6) Å) is normal. Hydrogen bonding between the P═O and the anthracenyl proton at C5 is possible in view of the C−O and H---O distances of 2.842 and 2.101 Å, respectively, and the C−H−O angle of 135.72°.

Regioselectivity of the Double Cyclometalations. The $^{31}P\{^1H\}$ NMR studies clearly show that the double cyclometalation of PAnP by $Pt(L)(OTf)_2$ is regioselective, as the intensities of the signals of the geometrical isomers are different. The relative intensities of the signals obtained from direct integration are essentially the same as those obtained from the inverse-gated ^1H-decoupling spectra and are used to obtain the ratios

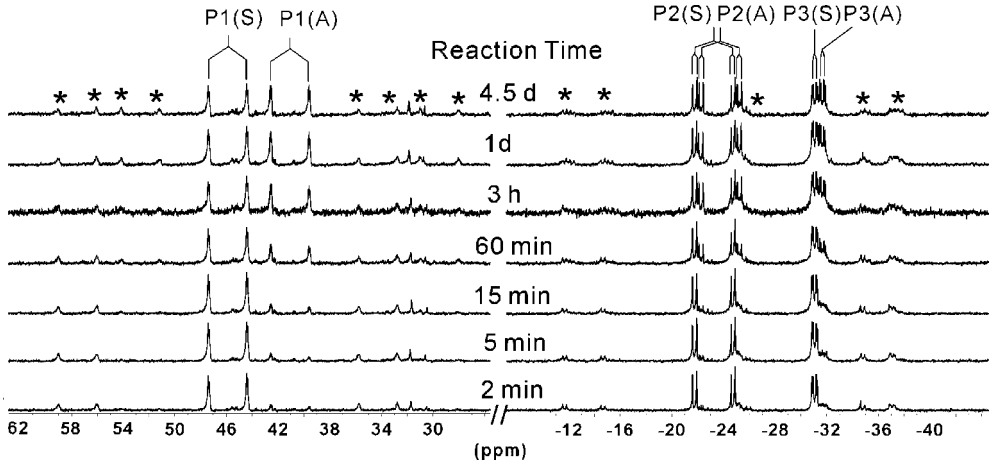

Figure 5. $^{31}P\{^{1}H\}$ spectra (CD_2Cl_2, 121.5 MHz) of products from reaction 1 in 100% CH_2Cl_2, showing the change of isomer distribution with reaction time. Peaks labeled as (S) are due to the *syn*-isomer **3a** and (A) the *anti*-isomer **3b**. * ^{195}Pt satellites.

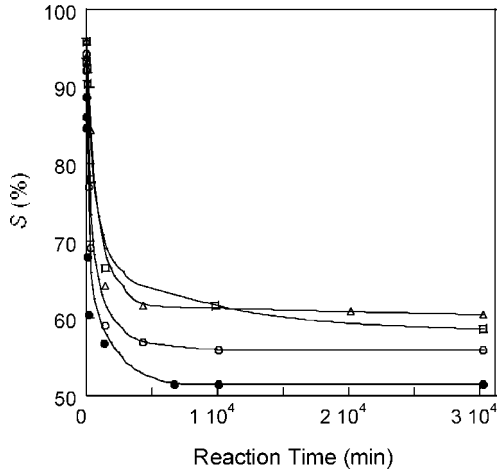

Figure 6. Change of the regioselectivity *S* of reaction 1 in CH_2Cl_2/CH_3CN solvent mixtures [CH_2Cl_2:CH_3CN v/v: 25:75 (Δ), 50:50 (□), 75:25 (○), 100:0 (●)] with time at room temperature.

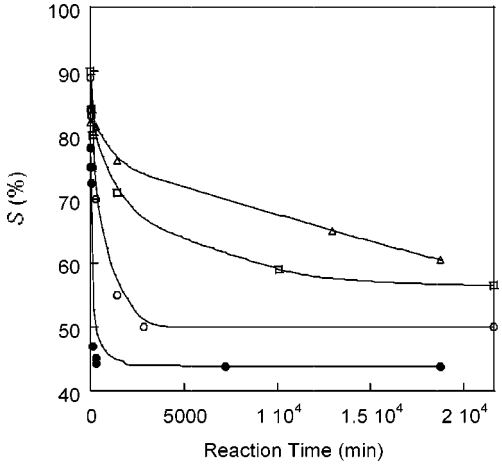

Figure 7. Change of the regioselectivity *S* of reaction 3 in CH_2Cl_2/CH_3CN solvent mixtures [CH_2Cl_2:CH_3CN v/v: 25:75 (Δ), 50:50 (□), 75:25 (○), 100:0 (●)] with time at room temperature.

of the isomers. The regioselectivity is defined as $S = [syn]/([syn] + [anti]) \times 100\%$, where [*syn*] and [*anti*] are the integrated intensities of the $^{31}P\{^{1}H\}$ NMR signals of the isomers, which are proportional to the concentrations of the complexes.

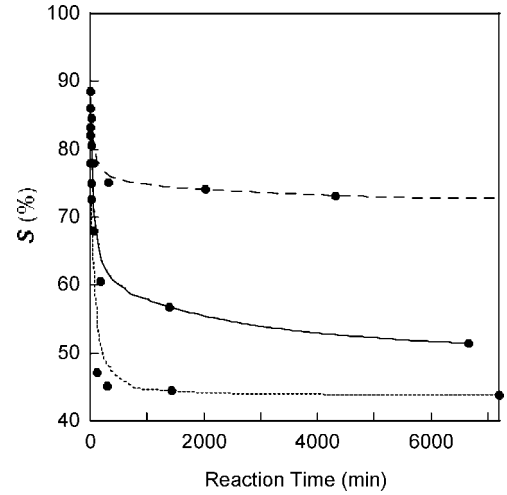

Figure 8. Change of the regioselectivity *S* of the double cyclometalation with time in CH_2Cl_2 at room temperature. Reaction 1: solid line. Reaction 2: dashed line. Reaction 3: dotted line.

Table 4. S_i and S_f for Reactions 1 and 3

	reaction 1		reaction 3	
CH_3CN % (v/v)	S_i	S_f	S_i	S_f
0	89	51	78	44
25	94	56	89	50
50	96	59	90	56
75	96	61	85	60

It was discovered that *S* changes with time as the two geometrical isomers undergo slow isomerization at room temperature. Typically an equilibrium is reached after 3−4 h. Figure 5 shows the $^{31}P\{^{1}H\}$ NMR spectral changes for reaction 1 in neat CH_2Cl_2. All three reactions exhibit an increase in the minor product, the *anti*-isomer, at the expense of the major product, the *syn*-isomer. It is clear that the cyclometalation is *reversible* (vide infra).

Since the isomerization is catalyzed by the protons released from the metalation of the C−H bond (vide infra), the *S* at different reaction times can be determined by quenching isomerization by addition of excess triethylamine. Figures 6 and 7 show respectively the variation of *S* of the reactions 1 and 3 in CH_3CN/CH_2Cl_2 mixtures (v/v = 0:100, 25:75, 50:50, and 75:25), and Figure 8 compares the *S* of the three reactions in neat CH_2Cl_2.

Scheme 3

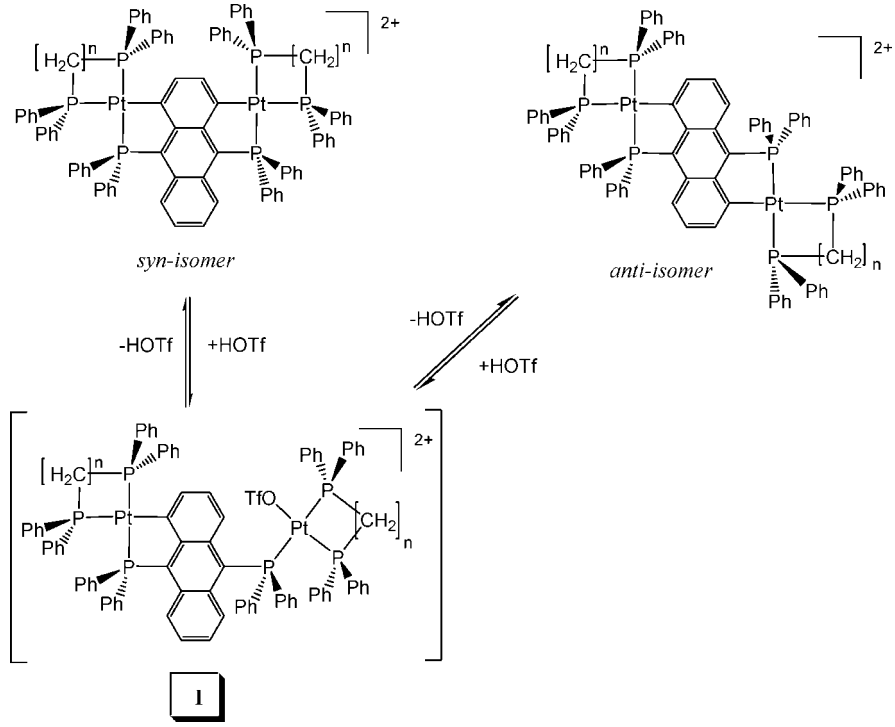

Table 5. $^{31}P\{^1H\}$ NMR (in CD_2Cl_2, 121.5 MHz) Data for I ($n = 3$)

	δ (ppm)	^1J(Pt−P) (Hz)	^2J(P−P) (Hz)
P1	48.17	2649	P1−P2 = 340
P2	8.44	2335	P2−P3 = 34
P3	−8.05	1780	P1−P3 = 15
P1A	27.83	2335	P1A−P2A = 332
P2A	−6.54	2266	[a]
P3A	2.54	3368	

[a] $^2J_{P2A-3A}$ and $^2J_{P1A-P3A}$ are unresolved.

Table 4 shows the regioselectivity for reactions 1 and 3 at a short reaction time (∼5 min) as well as at sufficiently long reaction time (1−2 weeks). The former is defined as the initial regioselectivity (S_i), and the latter is defined as the final regioselectivity (S_f).

All three reactions show a decrease in S in the first 5 h until an equilibrium is attained after a few days. The S_f is lower than the corresponding S_i. For reaction 1, the concentrations of *syn*- and *anti*-isomers are nearly the same (S_f = 51%) in CH_2Cl_2 after 4 days. For reaction 2 in CH_2Cl_2, **2a** remains the major product even though S decreases from 84% (S_i) to 73% (S_f) in 3 days. Reaction 3 in CH_2Cl_2 reaches thermal equilibrium in 24 h, much faster than the other two reactions, and unlike reactions 1 and 2, the major product is the *anti*-isomer (S_f = 44%). But increasing CH_3CN to 75% favors the formation of the *syn*-isomer as S_f is increased to 60%. In fact, for all three reactions, S_f increases with the percentage of CH_3CN in the solvent mixtures.

Scheme 3. is a proposed mechanism for the second cyclometalation and isomerization. The second cyclometalation should start with the coordination of the second Pt ion to the remaining free PPh_2 group of PAnP, forming an intermediate **I**. Subsequent attack of the second Pt ion at C4−H4 and C5−H5 leads to the *syn*- and *anti*-isomers, respectively. The formation of a Pt−C bond is accompanied with the release of a proton. The isomerization begins with the protonolysis of the Pt−C bond in the doubly cyclometalated complexes. The isomerization is acid-catalyzed, and it can be quenched by addition of excess NEt_3 as mentioned before.

Protonolysis. It has been demonstrated that the Pt−C bonds of some organoplatinum complexes can be cleavage by protonation (protonolysis).[10] According to the mechanistic proposal and on the basis of the reversibility of the cyclometalation, it is expected that the Pt−C bonds of the **Pt_2** complexes can be cleaved by acid. Addition of a slight excess of HOTf (∼1.2-fold) to solutions of **3a** and **3b** changes the $^{31}P\{^1H\}$ spectra of the compounds. Notably, both resulting spectra (SF1) are the same, consisting of two sets of signals of equal intensity that do not couple with each other. Each set of signal is composed of three mutually coupled P atoms in 1:1:1 ratio, and all signals are split by $^1J_{Pt-P}$ coupling. One set of the signals, labeled P1, P2, and P3, has chemical shifts and $^1J_{Pt-P}$ close to those of **3a** and **3b**, whereas the other set of signals, labeled P1A, P2A, and P3A, does not (Table 5). It is believed that the intermediate **I** shown in Scheme 3 is formed in the protonolysis. The signals that have chemical shifts and coupling constants very similar to those of **3a** and **3b** are assigned to P1, P2, and P3, which coordinate to the cyclometalated Pt ion. The other set of signals is ascribed to P1A, P2A, and P3A bonded to the dangling Pt ion. It is noted that the $^1J_{Pt-P3A}$ (3368 Hz) is exceptionally large, indicating that P3 is *trans* to a weak ligand, and accordingly it is assigned to the P atom opposite the OTf^- ion. The ^1H NMR signals of the complex are very broad and cannot be resolved at either 300 or 193 K. Similar spectra are obtained from the protonolysis of **1a**,**b** and **2a**,**b**.

Interestingly, removal of HOTf by adding excess Et_3N to the protonolyzed mixtures leads to disappearance of the signals of the intermediate and appearance of the signals of the doubly cyclometalated complexes with distribution of the isomers being

(10) (a) Romeo, R.; D'Amico, G. *Organometallics* **2006**, *25*, 3435. (b) Belluco, U.; Giustiniani, M.; Graziani, M. *J. Am. Chem. Soc.* **1967**, *89*, 6494. (c) De Felice, V.; De Renzi, A.; Panunzi, A.; Tesauro, D. *J. Organomet. Chem.* **1995**, *488*, C13−C14. (d) Hill, G. S.; Rendina, L. M.; Puddephatt, R. J. *Organometallics* **1995**, *14*, 4966. (e) Stahl, S. S.; Labinger, J. A.; Bercaw, J. E. *J. Am. Chem. Soc.* **1995**, *117*, 9371. (f) Cámpora, J.; López, J. A.; Palma, P.; Valerga, P.; Spillner, E.; Carmona, E. *Angew. Chem., Int. Ed.* **1999**, *38*, 147. (g) Lersh, M.; Tilset, M. *Chem. Rev.* **2005**, *105*, 2471.

Scheme 4

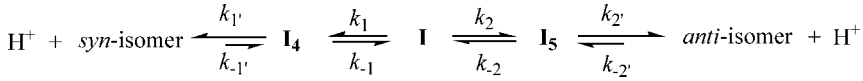

Scheme 5

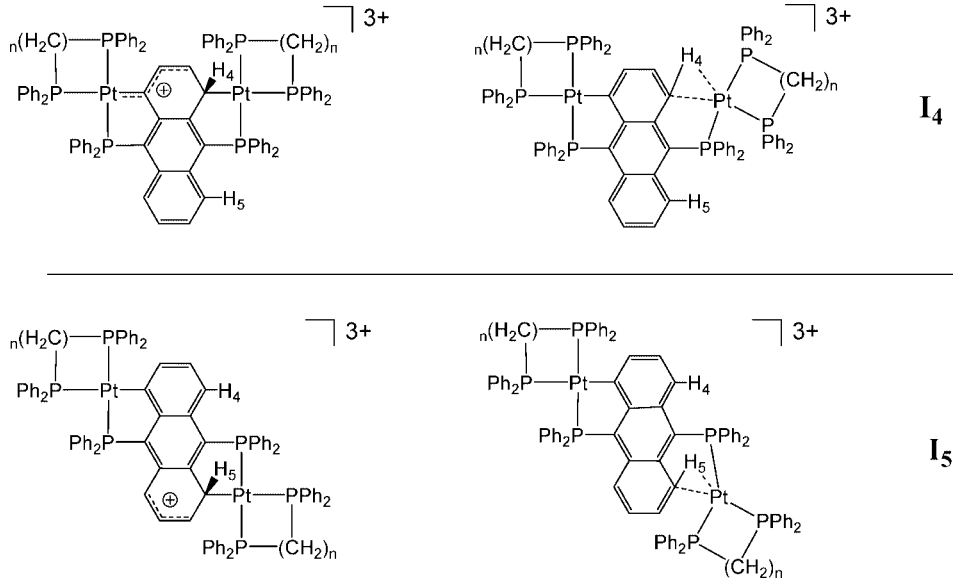

close to the S_f. This indicates that acid can speed up the isomerization and lends further support to the proposal that the intermediate **I** is formed in the protonolysis.

Mechanistic Postulate. As the cyclometalation is reversible, the final regioselectivtiy S_f should be the thermodynamic product distribution.[11] The S_f for reaction 1 in CH_2Cl_2 is 51%, indicating that the two isomers **1a** and **1b** are nearly isoenergetic. On the other hand, the S_f for reaction 3 in CH_2Cl_2 is 44%, meaning **3b** is slightly more stable than **3a**, by ~0.6 kJ mol^{-1}. These are very small free energy differences and could be caused by small differences in solvation energy or steric congestion between the isomers. A general observation is that the *syn*-isomer is more favored as the concentration of CH_3CN in the solvent mixture increases. It can be explained by the fact that the *syn*-isomer has a dipole moment larger than that of the *anti*-isomer, which has a center of inversion, and therefore can be better solvated in more polar solvent.

The S_i approximates the kinetically controlled product distribution. It ranges from 78% to 96%, indicating that the *syn*-isomers are the major kinetic products, and they are formed faster than the corresponding *anti*-isomers. It further implies that the attack of the second Pt ion to the C4−H4 bond is faster than to the C5−H5 bond. A reaction scheme is proposed to explain the regioselectivity (Scheme 4). Many studies on the mechanism of C−H bond activation by Pt(II) ion support the formation of an intermediate preceding the formation of the Pt−C bond and deprotonation.[1d,10g] Accordingly, the attacks of the Pt ion at the C4−H4 and C5−H5 bonds of the ring should lead to intermediates $\mathbf{I_4}$ and $\mathbf{I_5}$, respectively.

As both C−H bond activation and deprotonation are reversible, the regioselectivity can be affected by the rates of deprotonation as well as the proportions of $\mathbf{I_4}$ and $\mathbf{I_5}$. However, it is reasonable to assume that $k_{1'}$ and $k_{2'}$ should be similar. Accordingly, the kinetic product distribution should be mainly determined by the ratio of $\mathbf{I_4}$ and $\mathbf{I_5}$, which can be estimated by eq 1 ($[syn]_i/[anti]_i$ is the ratio of the isomers in kinetic distribution, and G_4 and G_5 are free energy of $\mathbf{I_4}$ and $\mathbf{I_5}$, respectively).[12]

$$\frac{[syn]_i}{[anti]_i} \approx \frac{[\mathbf{I_4}]}{[\mathbf{I_5}]} = \frac{k_1 k_{-2}}{k_{-1} k_2} = \exp\left(\frac{-(G_4 - G_5)}{RT}\right) \qquad (1)$$

That the *syn*-isomer is the major kinetic product implies $\mathbf{I_4}$ is more stable than $\mathbf{I_5}$. Assuming the steps $\mathbf{I} \rightarrow \mathbf{I_4}$ and $\mathbf{I} \rightarrow \mathbf{I_5}$ involve similar transition states, the stability of $\mathbf{I_4}$ and $\mathbf{I_5}$ should correlate with the exothermicity of the two steps. In other words, the C4−H4 bond in **I** should be more reactive than the C5−H5 bond. If the C−H activation goes through an electrophilic pathway, then one would expect the C4−H4 bond to be more electron-rich than the C5−H5 bond. On the other hand, if the reaction goes through a nucleophilic pathway, the C4−H4 bond should be more electron-deficient than the C5−H5 bond. It does not necessarily mean that the two positions must be greatly different in terms of electron density. In fact, the S_i of 96% observed for reaction 1 in 25:75 CH_2Cl_2/CH_3CN can be accounted by an energy difference of only ~8 kJ mol^{-1} between the two intermediates.

The electronic effect of the first Pt ion clearly directs the second attack. Unfortunately, the ^{1}H NMR spectra of the intermediate **I** formed by protonolysis cannot be resolved. Nonetheless, the mononuclear complexes **4** and **5** could provide some clues about the different reactivity of the two C−H bonds in **I**. For both complexes, H4 is more upfield than H5: the two protons are different by 0.24 ppm (**4**) and 0.44 ppm (**5**). Similarly, the HMQC spectra of the complexes show that C4 is more upfield than C5 by ~3 ppm in both complexes (SF2 and 3). These suggest that the C4−H4 bond is more electron-rich than the C5−H5 bond. Accordingly, an electrophilic pathway is more consistent with the preferential attack of the second Pt ion at the C4−H4 bond. $\mathbf{I_4}$ and $\mathbf{I_5}$ could be

(11) Berson, J. A. *Angew. Chem., Int. Ed.* **2006**, *45*, 4727.

(12) (a) Curtin, D. Y. *Rec. Chem. Prog.* **1954**, *15*, 111. (b) Hammett, L. P. *Physical Organic Chemistry*; McGraw-Hill: New York, 1970; Chapter 5. (c) Seeman, J. I. *J. Chem. Educ.* **1986**, *63*, 42.

σ-complexes (Scheme 5, left), which have the Pt ion bonded to either the carbon atom (Wheland intermediate)[1c,13] or the C−H bond, forming an agnostic complex (Scheme 5, right).[14] For both cases, the formation of $\mathbf{I_4}$ is favored over that of $\mathbf{I_5}$ by the π-back-donation from the first Pt ion.

Conclusion

This study demonstrated the double cyclometalation of PAnP is regioselective and revealed a rather complicated mechanistic picture of the seemingly simple reaction. The regioselectivity can be influenced by the solvent and the ancillary diphosphine ligands. The *syn*-isomers are the kinetic products, but the reaction is thermodynamically controlled, as the isomers can undergo acid-catalyzed isomerization. The proposed mechanistic model invokes a preferential electrophilic attack of the second Pt ion at the C4−H4 and C5−H5 bonds of the anthracenyl ring, producing two intermediates, $\mathbf{I_4}$ and $\mathbf{I_5}$. Subsequently deprotonations lead to the *syn*- and *anti*-isomers, respectively.

Acknowledgment. The authors would like to thank National University of Singapore and Ministry of Education Singapore (R-143-000-331-112) for financial support and Miss Tan Geok Kheng for determining the X-ray crystal structures.

Supporting Information Available: Crystallographic data, CIF files of **2a**, **2b**, and **5**, HMQC spectra of **4** and **5**, and $^{31}P\{^1H\}$ NMR spectrum and data for **I**. This material is available free of charge via the Internet at http://pubs.acs.org.

OM800356K

(13) (a) Sweet, J. R.; Graham, W. A. G. *Organometallics* **1983**, *2*, 135. (b) Albrecht, M.; Dani, P.; Lutz, M.; Spek, A. L.; van Koten, G. *J. Am. Chem. Soc.* **2000**, *122*, 11822. (c) Davies, D. L.; Donald, S. M. A.; Macgregor, S. A. *J. Am. Chem. Soc.* **2005**, *127*, 13754. (d) Shilov, A. E.; Shul'pin, G. B. *Chem. Rev.* **1997**, *97*, 2879. (e) Singh, A.; Sharp, P. R. *J. Am. Chem. Soc.* **2006**, *128*, 5998.

(14) (a) Vigalok, A.; Uzan, O.; Shimon, L. J. W.; Ben-David, Y.; Martin, J. M. L.; Milstein, D. *J. Am. Chem. Soc.* **1998**, *120*, 12539. (b) Johansson, L.; Tilset, M.; Labinger, J. A.; Bercaw, J. E. *J. Am. Chem. Soc.* **2000**, *122*, 10846. (c) Stahl, S. S.; Labinger, J. A.; Bercaw, J. E. *J. Am. Chem. Soc.* **1996**, *118*, 5961. (d) Heiberg, H.; Johansson, L.; Gropen, O.; Ryan, O. B.; Swang, O.; Tilset, M. *J. Am. Chem. Soc.* **2000**, *122*, 10831. (e) Kua, J.; Xu, X.; Periana, R. A.; Goddard, W. A., III. *Organometallics* **2003**, *21*, 551. (f) Thomas, J. C.; Peters, J. C. *J. Am. Chem. Soc.* **2001**, *123*, 5100. (g) Tellers, D. M.; Yung, C. M.; Arndtsen, B. A.; Adamson, D. R.; Bergman, R. G. *J. Am. Chem. Soc.* **2002**, *124*, 1400.